American Journal of Engineering and Applied Sciences

Original Research Paper

Defect Classification of Reinforced Concrete Structures with Nondestructive Tests Using Statistical and Machine Learning Methods

[1]Sajjad Sayyar-Roudsari, [1]Armaghan Shalbaftabar, [2]Farshid Damirchilo, [3]Rohollah Taslimian, [4]Taher Abu-Lebdeh, [4]Sameer Hamoush and [5]Sun Yi

[1]Department of Computational Science and Engineering, North Carolina A and T State University, Greensboro, NC, USA
[2]Ira A. Fulton Schools of Engineering, Arizona State University, Tempe, AZ, USA
[3]Department of Civil Engineering, Louisiana Tech University, Ruston, LA, USA
[4]Department of Civil, Architectural and Environmental Engineering, North Carolina A and T State University, Greensboro, NC, USA
[5]Department of Mechanical Engineering, North Carolina A and T State University, Greensboro, NC, USA

Article history
Received: 24-01-2024
Revised: 19-02-2024
Accepted: 27-03-2024

Corresponding Author:
Sajjad Sayyar-Roudsari
Department of Computational Science and Engineering, North Carolina A and T State University, Greensboro, NC, USA
Email: ssayyarroudsari@aggies.ncat.edu

Abstract: In this study, twelve reinforced concrete beams were constructed, each with specified dimensions and initial compressive strength. The beams were divided into four groups: A control group without any defect, a void group featuring a centrally located void, a corrosion group and a debonding group. The impact echo test was used for nondestructive testing, gathering data on compressive and shear wave velocity and frequency. The collected data, including compressive and shear wave velocity, frequency and derived material properties as well as modulus of elasticity, were used for subsequent analyses. To determine the type of defect, artificial intelligence and machine learning methods were utilized. Data collected from the impact echo method were analyzed using RStudio and the MATLAB toolbox for statistical analysis. Linear regression was employed to establish relationships between inputs (wave velocity and frequency) and outputs as shear and compressive modulus. The accuracy of these relationships was assessed through correlation coefficients, p-values and adjusted R-squared error. Additionally, an Imperial Competitive Algorithm (ICA) as part of the artificial neural network method was implemented to predict the variables. The results demonstrated high correlation coefficients and low mean square errors, indicating accurate predictions. Frequency domain defect detection was performed by analyzing frequency-amplitude data. The MATLAB toolbox was used to identify peaks and determine defects based on a 20% boundary condition. The comparison of peaks confirmed the presence of defects in beams with voids, corrosion and debonding. Subsequently, support vector machines were employed to classify defects in reinforced concrete structures, including voids, corrosion and debonding. This study utilized key features of reinforced concrete and assessed SVM performance using precision, recall and F1-score metrics. Overall, this study illustrates the effectiveness of machine learning techniques complied with impact echo tests in assessing and predicting the quality of reinforced concrete beams with various internal defects.

Keywords: Non-Destructive Tests, Defect Classification, Machine Learning, Artificial Neural Network, Imperial Competitive Algorithm, Support Vector Machine

Introduction

Nondestructive Testing (NDT) methods have become a prevalent approach for assessing infrastructures and structures, particularly reinforced concrete structures (Johnson and Pessiki, 1993; Lopes and Nepomuceno, 1997; Collins, 1995). The NDT method not only facilitates the characterization of material properties in concrete structures but also offers insights into visualizing the overall quality of the concrete (Nepomuceno and Lopes, 2017; Beben *et al*., 2013). In terms of material properties, frequency domain data is derived from signal processing and sound vibration analysis, with visualization relying on a laser-based approach (Carino, 2001; Hoła and Runkiewicz, 2018; Hugenschmidt, 2002; Rehman *et al*., 2016).

Oh *et al*. (2023) used Impact Echo (IE) to detect defects of prestressed concrete. He introduced a cost-effective technique for identifying voids within ducts in Prestressed Concrete (PSC) bridges, which were prone to corrosion and structural failure if the tendon within the duct corrodes. Conventional methods, such as Non-Destructive Testing (NDT) utilizing ultrasonic waves, were both costly and required skilled personnel. Instead, the authors propose utilizing an Impact Echo (IE) method combined with Deep Support Vector Data Description (Deep SVDD). This method distinguished data as either normal or defective by employing a hypersphere in a multi-dimensional feature space created by an autoencoder. The autoencoder, modeled after Embeddings from Language Model (ELMo), efficiently represents IE data. Experimental findings illustrate the effectiveness of the model, achieving an accuracy rate of roughly 77.84%, marking a notable enhancement compared to supervised learning approaches by approximately 47%.

Hong *et al*. (2020) used the ultrasonic pulse velocity method to evaluate reinforced concrete structures.

The research aimed to predict the compressive strength of concrete structures as they aged using the ultrasonic pulse velocity method. Establishing a relationship between ultrasonic pulse velocity and compressive strength over time was intended to assist in estimating the compressive strength of newly constructed buildings or those undergoing renovation. The study involved fabricating 123 concrete specimens with varying parameters, including design compressive strengths ranging from 24-40 MPa at different ages (16-672 h). Ultrasonic velocity measurements were conducted following standardized procedures and compressive strength was determined accordingly. By examining the correlation between ultrasonic pulse velocity and compressive strength, the study proposed an equation for estimating compressive strength based on age, demonstrating the potential of using nondestructive testing methods for this purpose.

The IE method is a powerful Non-Destructive Testing (NDT) technique widely used for assessing the condition of concrete structures. However, it comes with certain limitations that can impact its effectiveness in certain scenarios. One significant limitation is related to the size and shape of defects that can be detected. While IE is adept at identifying large defects such as voids, delamination and cracks, it may struggle to detect smaller defects or those located at deeper depths within the concrete structure. This limitation can be particularly challenging when assessing structures with complex geometries or those where defects are distributed across different depths.

Another limitation of the IE method is its reliance on access to both sides of the concrete elements being tested. In situations where access to one side of the structure is restricted or impossible, such as in the case of heavily reinforced concrete or structures with limited entry points, conducting impact-echo testing becomes impractical. This constraint restricts the method's applicability in real-world scenarios where complete access to the structure may not be feasible. Additionally, the accuracy of IE results can be influenced by factors such as surface roughness, moisture content and the presence of reinforcing bars, further adding to the complexity of its application and interpretation in concrete NDT.

Zhao *et al*. (2018) utilized ultrasonic nondestructive test methods to assess defect determination in reinforced concrete structures. Six reinforced concrete components with varying defect levels were fabricated. Data acquisition involved Piezoceramic Transducers (PT) and the Time Reversal Method (TRM) to generate time-frequency graphs. Defect visualization was achieved through the image processing toolbox. The results displayed the location of the internal defect with reasonable accuracy. Atamturktur (2011) conducted experimental and analytical investigations on intentionally defective reinforced concrete (Damirchilo *et al*., 2021) beams. The finite element method was employed to simulate frequency tests and Bayesian calibration techniques were applied for comparison with experimental samples. The results demonstrated that the defect detection by this method may not be accurate enough when compared with experimental tests due to several factors.

Brilakis *et al*. (2011) studied the Visual Pattern Recognition (VPR) of infrastructures. The VPR has been used by the image analysis toolbox to take detailed information about the image. The result indicated that this method could distinguish the air pocket on the concrete surface. Dawood *et al*. (2018) explored the application of a computer vision model for identifying moisture locations in subways. They utilized an artificial neural network alongside the Red-Green-Blue (RGB) method for visualization to reduce noise. Their findings showcased that combining the RGB and ANN methods optimized moisture detection capabilities. Additionally, reinforced concrete structures might exhibit internal issues such as corrosion, deterioration, delamination, voids and more (Nanekar *et al*., 2019; Sadowski, 2022; Cotič *et al*., 2018). Sugimoto *et al*. (2018) employed statistical analysis to detect the internal defects of concrete structures. They utilized a non-contact device, a long-range acoustic device, as well as a laser Doppler vibrometer to distinguish good quality parts from poor ones. The investigation involved testing on concrete slabs of both bridges and railroad tunnels. The examination centered on the application of spectral entropy and corresponding frequency peaks to ascertain concrete quality by identifying the presence or absence of resonance peaks in frequency graphs.

Shah *et al*. (2012) studied the integration of non-linear ultrasonic techniques with Artificial Neural Networks (ANNs) to assess damages in stressed concrete non-destructively is explored in the study. Two ANN models, one utilizing raw data and the other employing dimensionless variables, were developed and tested for predicting concrete damage. Input data for the ANN consisted of time-domain signals from ultrasonic waves, gathered from previous experimental studies involving 75 ultrasonic measurements on concrete cubes with varying water-cement ratios. Both ANN models were two-layer perceptrons trained using the back-propagation algorithm. The potential of ANN in evaluating concrete damage using non-linear ultrasonic measurements is demonstrated by the results. The proposed ANN models exhibit low absolute errors in predicting concrete cube strength, with the model utilizing raw data being outperformed by the one using grouped dimensionless variables.

Automated flaw detection in concrete using ultrasonic tomography and Convolutional Neural Networks (CNN) was explored in Marek Słoński's study (Słoński *et al*., 2020). The methodology involved obtaining images through ultrasonic tomography and utilizing CNN to automatically detect defects. The model, fine-tuned on laboratory test images, accurately identified defects in concrete elements. This automated approach has the potential to classify various defect types in concrete.

Jiang *et al*. (2024) conducted a study on identifying multiple cracks in large structures using a novel data-driven algorithm combining the Scaled Boundary Finite Element Method (SBFEM) and deep learning techniques. Quantifying structural defects accurately is challenging, prompting the development of this innovative approach. The algorithm integrates SBFEM to simulate various crack-like defects, simplifying mesh generation and minimizing re-meshing efforts. An absorbing boundary model with Rayleigh damping is utilized for efficient wave propagation simulation in massive structures. To enhance the neural network's ability to capture sequential data and complex mapping relationships, a dilated causal Convolutional Neural Network (CNN) is employed. This enables the model to accurately detect the number, location and depth of cracks while remaining robust to noise. The proposed algorithm holds promise for enhancing structural defect detection and diagnosis, thereby enhancing overall engineering structure safety.

Kuchipudi and Ghosh (2024) developed a method for the automated detection and segmentation of internal defects in reinforced concrete using deep learning on ultrasonic images. While periodic inspection of concrete structures was recommended for ensuring safety, manually screening ultrasonic images for defects had been laborious and error-prone. The study proposed a region-based CNN to automatically detect, localize and segment defects in ultrasonic images. The network, which was trained on real experimental data, employed the synthetic aperture focusing technique to generate an ultrasonic image dataset containing various defects like debonded rebars and cracks. The model achieved a high mean Average Precision (mAP) of 0.98 in detecting and masking defect pixels, surpassing other state-of-the-art defect detection networks.

Many researchers studied the effect of using nondestructive tests to determine the quality of existing reinforced concrete structures. Most of these researchers focused on experimental tests or numerical analyses to evaluate the quality of reinforced concrete structures. Further, a few researchers studied machine learning methodologies to determine concrete defects. Despite numerous studies, none have addressed the methodology of classifying and detecting types of defects in existing reinforced concrete structures using numerical techniques. Also, no study has been conducted to show how to predict different types of defects based on impact echo results and statistical analysis with machine learning techniques.

In this study, diverse reinforced concrete beams were made in the laboratory. These beams were constructed in four groups including no defect, void, corrosion and debonding. Impact echo is employed to perform testing and collect data. Then, statistical analyses including linear regression, artificial neural network and machine learning methods are employed to evaluate the IE data and classify the defect's type accordingly.

Experimental Investigation

In this study, twelve reinforced concrete beams have been constructed in the structural lab (Sayyar-Roudsari *et al*., 2020; Roudari *et al*., 2020; Roudsari, 2020). The beam's dimensions are 8×16×96 inches in width, height and length respectively. The initial concrete compressive strength is computed to be at least 4000 Psi. RC beams are divided into four groups and each group has three specimens. The first group is the control group (group A) meaning that there is no internal defect. The second group is subjected to have void (group B) located at the center of RC beams. The location of the void is about 48 inches from the edge and 3 inches from the top surface of the RC beam. The geometry of the void is also 3×2×1 inches in height, width and thickness. The third group is corrosion (group C) and the fourth one is debonding (group D). It needs to be mentioned that corroded bars are made by a natural process where bars are immersed in a water pond for a few months and debonding is implemented by fully lubricating bars. Four numbers of #4 have been employed at the tensile area of the RC beam. Figures 1-2 show the geometry and actual RC beams. Table. 1 displays the group names based on different defects (Sayyar-Roudsari *et al*., 2020; Roudari *et al*., 2020; Roudsari, 2020).

Table 1: RC beams group name, ID (Sayyar-Roudsari *et al*., 2020; Roudari *et al*., 2020; Roudsari, 2020)

Group name type	A Control			B Void			C Corrosion			D Debonding		
ID	A1	A2	A3	B1	B2	B3	C1	C2	C3	D1	D2	D3

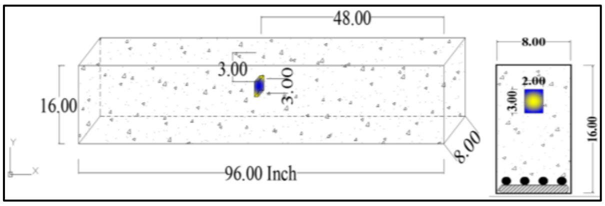

Fig. 1: Geometrical properties of RC beam (Sayyar-Roudsari *et al*., 2020; Roudari *et al*., 2020; Roudsari, 2020)

Fig. 2: RC beam in the structural lab (Sayyar-Roudsari *et al*., 2020; Roudari *et al*., 2020; Roudsari, 2020)

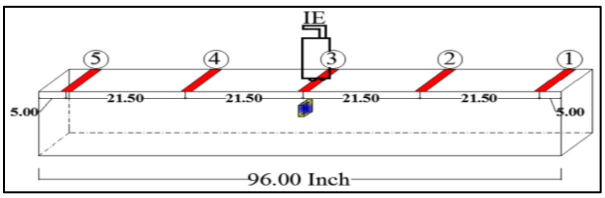

Fig. 3: Impact echo test's locations on RC beam

In order to collect data, the impact echo as a nondestructive test method is employed. This device uses ultrasonic methods which are based on an acoustic base system (Taslimian *et al*., 2023). The IE device is used to run on the top surface of the RC beam and several tests are performed on each location to collect data. These tests are done in five different locations for each RC beam which is shown in Fig. 3. The IE test carries out the results for each spot and data from each test is collected for the analysis scheme.

The fundamental properties of a medium, particularly shear wave velocity and compressive wave velocity, significantly influence the dispersion properties of waves (Taslimian *et al*., 2015; 2012; Ross and Willson, 2018). The impact echo test can give information like compressive and shear wave velocity as well as compressive and shear wave frequency. Based on this data, the module of elasticity, shear modulus and compressive strength of concrete are computed.

Materials and Methods

The concrete mixtures employed for the experimental tests were based on ASTM C494 and ASTM C1017 standards. The concrete exhibits a compressive strength of 4000 psi (27.58 MPa) with a water-to-cement ratio (w/c) of 0.5, resulting in a slump of 4 inches (101.6 mm). Self-Consolidating Concrete (SCC) was utilized to address vibration issues, such as aggregate blockage. For reinforcement, Grade 40 steel bars measuring 0.5 inches (12.7 mm) in diameter were utilized. These bars exhibit yield and ultimate strengths of 40000 and 70000 psi (275.80 and 482.63 MPa) respectively, in accordance with ASTM A615 standards.

One crucial criterion for a statistical approach is ensuring a sufficient amount of data. Utilizing IE provides a large data set as input and output parameters of each specimen. Table 2 displays the initial four columns obtained by executing the IE software, wherein compressive wave velocity, shear wave velocity, compressive frequency and shear frequency serve as the input data. The IE software records data through vibrations, capturing both frequency and velocity. On the other hand, Young's modulus, shear modulus and compressive strength are calculated from the provided input data.

To establish relationships between inputs and outputs, the linear regression method is employed using RStudio software. Specifically, the compressive frequency category is chosen to assess linearity for the modulus of elasticity and compressive strength. Moreover, the correlation between compressive wave velocity and compressive frequency is investigated. The selection of polynomial degrees of freedom is crucial for linear regression, where input and output data are designated as independent and dependent variables, respectively (Jäntschi *et al*., 2015). Notably, higher compressive frequency or velocity tends to correlate with increased compressive strength, emphasizing their significance in concrete quality assessment. Similarly, shear frequency and velocity are compared with shear modulus. In the broader context, the method for evaluating concrete quality often revolves around compressive strength, implying that a higher compressive frequency domain or velocity corresponds to better concrete quality. Equation 1 represents the general relationship between independent and dependent variables (Deschepper *et al*., 2006):

$$Y = Intercept + \beta\ (X) + \hat{\varepsilon} \tag{1}$$

Table 2: Data of impact Echo test

Beam type and spot's test	Compressive wave velocity	Shear velocity	Compressive frequency (Hz)	Shear frequency (Hz)	Young's modulus (Ksi)	Shear (Ksi)	Compressive strength (Psi)
A1-3	12444	7283	4667	2758	5023	1720	6865
B1-3	6932	4245	2600	1608	1559	0585	0661
C1-3	9646	6138	3617	2325	3017	1222	2477
D1-3	8468	5413	3175	2050	2325	0950	1471

The significant level (p-value) of all regression models is 0.05. The null hypothesis *(H_0)* indicates that the slop (β) is equal to zero and the alternative hypothesis *(H_a)* means that the slop (β) is not equal to zero. The observed errors ($\hat{\varepsilon}$) are named as residual meaning the difference between the fitted observed dependent (Y) and predicted values ($\hat{Y}$). Eq.2 displays the residual error of the dependent and independent models (Pogliani and Julián-Ortiz, 2005):

$$\hat{\varepsilon} = Y_i - \hat{Y}_i \tag{2}$$

The linearity assumption can be assessed through the residual plot, which indicates whether the model exhibits a random distribution pattern. A random distribution pattern suggests linearity, while a non-random pattern signifies nonlinearity (Iván and Carlos, 2015). Additionally, the QQ-Plot is utilized to verify the uniformity and normal distribution of the data, with a straight-line pattern indicating uniformity (Akossou and Palm, 2013). Linear regression involves two types of errors, namely R-squared and adjusted R-squared. A higher percentage value in these errors signifies more accurate results and their computation is outlined in Eqs. 3-4: (Van Trees and Bell, 2007):

$$R^2 = 1 - \frac{\sum_i^n (Y_i - \hat{Y}_i)^2}{\sum_i^n (Y_i - \bar{Y}_i)^2} \tag{3}$$

$$R^2_{adj} = 1 - \frac{MSE}{MST} \tag{4}$$

In these equations, $\bar{Y}_i$ is the mean of Y, the mean squared error is computed by $MSE = \frac{\sum_i^n (Y_i - \hat{Y}_i)^2}{(n-q)}$ and the sum of the squared total is $SST = \frac{\sum_i^n (Y_i - \bar{Y}_i)^2}{(n-1)}$, where *n* and q are the number of observation and the number of coefficients, in order. The standard error deviation formula is the square root of the mean square error which is displayed in Eq. 5:

$$Std.Error = \sqrt{MSE} \tag{5}$$

The F-statistic is calculated by $\frac{MSR}{MSE}$ where the MSR formula is shown in Eq. 6. (Kaveh and Talatahari, 2010):

$$MSR = \frac{\sum_i^n (Y_i - \bar{Y}_i)}{q-1} \tag{6}$$

To determine the linearity of parameters, RStudio is employed. In this software, data is imported with the "dataset" library. After importing data, each data category is separately divided and called out for linear regression. The "lm" command is utilized to create the regression model and the polynomial command is used to show two degrees as a quadratic model. To represent the residual analysis, linear regression is compiled with identical matrix (I) multiple (according to the dataset) $^{\wedge 2}$ such as lm (compressive_velocity~compressive_frequency + I (compressive_velocity $^{\wedge 2}$), data = CWVCF). CWVCF is an example of a data set to show as abbreviated stands for compressive wave velocity and compressive frequency, in order.

Further, for the Q-Q plot in RStudio, the qq norm () function is used to create the plot, passing the dataset as an argument. Then, a reference line for better interpretation is considered by adding the qq line () command. Executing the Q-Q plot compares the quantiles of the dataset against a theoretical distribution, aiding in assessing the dataset's conformity.

In this study, the Artificial Neural Networks (ANN) method is employed for the decision-making scheme.

Using Artificial Neural Networks (ANNs) for decision-making in defect detection of concrete offers several advantages. ANNs excel in handling complex and multidimensional data, making them suitable for tasks involving various parameters like texture, color, composition and structural properties. They can capture intricate patterns and relationships among these parameters, which is crucial for detecting subtle defects that may not be easily discernible using traditional methods. Additionally, ANNs can learn from historical data without relying heavily on predefined rules or linguistic terms, unlike fuzzy logic systems. This data-driven approach allows ANNs to adapt to different types of defects and environmental conditions, enhancing their robustness and generalization capability. ANNs also offer flexibility in model architecture, accommodating different network structures based on the nature of the input data and the complexity of the defect detection task. While fuzzy logic has been applied in various engineering domains for decision-making under uncertainty, its application in concrete defect detection may be limited due to factors such as interpretability versus complexity, handling non-linearity and limited learning capability compared to ANNs. In summary, while both ANNs and fuzzy logic have their strengths and weaknesses, ANNs are often preferred for defect detection in concrete due to their ability to learn complex patterns from data, handle non-linear relationships and adapt to diverse defect detection scenarios. However, the choice between these methods ultimately depends on the specific requirements of the application, the availability of training data and the desired balance between interpretability and predictive performance.

One of the most reliable methods in ANN is the Imperial Competitive Algorithm (ICA). The algorithm maintains a population of candidate solutions, each representing a potential solution to the optimization problem. These solutions are typically encoded as vectors in a multidimensional search space. In ICA, each candidate solution is classified as either an imperialist or a colony. Imperialist solutions represent dominant and influential entities, while colony solutions represent less influential entities. The algorithm starts with an initial population of candidate solutions. These solutions are randomly generated within the search space. Initially, a subset of these solutions is selected as imperialists, while the remaining solutions become colonies. During each iteration of the algorithm, imperialist nations compete for dominance over colonies. Imperialist nations with higher fitness (better solutions) are more likely to conquer colonies with lower fitness. This process reflects the socio-political concept of imperialism, where stronger nations tend to dominate weaker ones. Colonies assimilate into the empires of the victorious imperialist nations. This assimilation process involves updating the position of colonies towards the position of their corresponding imperialist nation. This allows colonies to benefit from the superior solutions found by their imperialist rulers. To maintain diversity and prevent premature convergence, a revolution process is incorporated into ICA. During a revolution, a fraction of colonies may rebel against their imperialist rulers and become independent solutions. This helps in exploring new regions of the search space and avoiding stagnation. After each iteration, the fitness of all candidate solutions is evaluated based on the objective function of the optimization problem. Imperialist nations and colonies are selected for the next iteration based on their fitness, with higher fitness solutions being more likely to survive and reproduce. The algorithm terminates when a stopping criterion is met, such as reaching a maximum number of iterations or achieving a satisfactory solution. The imperialist competitive algorithm has been successfully applied to various optimization problems, including engineering design, scheduling and data mining. Its ability to balance exploration and exploitation, along with its parallelism and scalability, makes it an effective optimization tool for solving complex problems.

While the Imperialist Competitive Algorithm (ICA) presents several advantages in optimization problem solving, it also has limitations. The performance of ICA can be sensitive to its parameters, such as the initial population size, the rate of revolution and the selection mechanism. Poorly chosen parameter values may lead to suboptimal convergence or premature convergence to local optima. ICA may exhibit slower convergence rates compared to some other optimization algorithms, especially in high-dimensional or complex search spaces. This can result in longer computational times, particularly for problems with large-scale data or intricate solution landscapes. While ICA incorporates a revolution process to promote exploration, it may still suffer from limited exploration capabilities, particularly in highly rugged or multimodal search spaces. The algorithm's exploration efficiency can be influenced by factors such as the selection mechanism and the degree of diversity in the population. Like many population-based optimization algorithms, ICA may encounter challenges in handling constraints effectively. Ensuring that candidate solutions satisfy all problem constraints can be non-trivial, especially when dealing with complex constraints or discontinuous feasible regions.

Despite these limitations, the Imperialist Competitive Algorithm can be suitable for defect detection in concrete due to several factors. Defect detection in concrete often involves optimizing multiple parameters or features simultaneously, such as texture, color, composition and structural properties. ICA's ability to handle multidimensional optimization makes it well-suited for addressing complex defect detection tasks. ICA aims to find globally optimal solutions by balancing exploration and exploitation. In defect detection applications, where the goal is to identify defects accurately and reliably across different concrete samples or structures, the ability to search for global optima is crucial. ICA's adaptability to different types of data and solution spaces makes it versatile for defect detection tasks. It can accommodate diverse data sources, including sensor readings, imaging data, or material properties and adjust its search strategy accordingly. Concrete defect detection often involves dealing with noisy or imperfect data, such as variations in surface conditions or environmental factors. ICA's robustness to noisy data and its ability to converge to robust solutions make it suitable for handling such challenges in defect detection applications.

Overall, while the imperialist competitive algorithm has limitations, its strengths in multidimensional optimization, global optimization capability, adaptability to data characteristics and robustness to noisy data make it a promising approach for defect detection in concrete. However, careful parameter tuning and consideration of problem-specific constraints are essential for achieving optimal performance in real-world applications.

In this research, MATLAB is utilized to develop the ICA codes. The code is written in a multi-algorithm file format to help faster and feasible analysis. This MATLAB code implements the Imperialist Competitive Algorithm

(ICA) for optimizing a given cost function. The code first sets up the problem parameters, including the name of the cost function, the network structure and the search space boundaries. It then initializes the algorithmic parameters, such as the number of countries, initial imperialists and the number of decades for the optimization process. The main loop of the algorithm iterates over a specified number of decades, during which it performs assimilation, revolution, empire possession and imperialistic competition operations. Additionally, the code includes options for plotting the evolution of imperialists and the minimum and mean costs over the iterations. Finally, the algorithm terminates after the specified number of decades and it returns the best network and its corresponding cost. This code is suitable for optimizing the parameters of a neural network model for defect detection in concrete, as it efficiently explores the solution space and balances exploration with exploitation, potentially leading to improved detection accuracy and robustness.

Moreover, the MATLAB toolbox is exploited to define the artificial neural network (Hugenschmidt, 2002) method for predicting the data of dependent and independent variables. Although there are special functions in MATLAB to define the neural network algorithm, a very specific method Imperial Competitive Algorithm (ICA) is used to write and define all parameters, exclusively. In the Imperial Competitive Algorithm (ICA) method, random samples are generated. Each sample is called a country (Mohammadi-Ivatloo *et al*., 2012; Vapnik, 1998). The instruction of ICA is as follows:

- ✓ Each sample is called a country
- ✓ Countries (samples) are divided into two main groups
  - o Imperialist: Imperialist countries control the colonies based on their power
  - o Colony: Each imperialist has some colonies according to the powerfulness

The Imperialist Competitive Algorithm (ICA) is employed to train a neural network model using the provided dataset. The dataset consists of input features and corresponding output values. Initially, the data was preprocessed, including normalization of input and output variables to ensure consistent scaling across the dataset. The dataset was then divided into training and testing sets, with 80% of the data used for training and the remaining 20% for testing.

For the neural network architecture, a feedforward neural network with two layers is constructed, comprising five neurons in the hidden layer and the number of output neurons corresponding to the number of output variables. The training goal for the network was set at 0.0001 to optimize the network's performance.

After training the neural network using the ICA algorithm, the model's performance is assessed on both the training and testing datasets. The Mean Squared Error (MSE) is calculated to evaluate the model's accuracy, with lower MSE values indicating better performance. Additionally, the correlation coefficient is computed to assess the relationship between the actual and predicted output values, with values closer to 1 indicating stronger correlations.

Results and Discussion

In this study, a linear regression plot is used to explore the relationship between two continuous variables. It depicts how a dependent variable changes with respect to an independent variable. In a linear regression plot, data points are typically scattered around a straight line, which represents the best-fitting linear relationship between the variables. The slope of the line indicates the strength and direction of the association between the variables, while the intercept represents the value of the dependent variable when the independent variable is zero. Additionally, the plot may include confidence intervals or prediction intervals around the regression line to assess the uncertainty of the estimated relationship.

Figure 4 shows the linear regression of compressive strength versus compressive frequency. As it is obvious, the correlation coefficient of this model is about 98%, indicating a high accuracy of the result. Equation 7 indicates the relationship between dependent and independent variables of compressive strength and frequency. In order to check the accuracy of this relationship, the p-value is compared to the significant level. The result section of Fig. 4 shows the p-value is $2e^{-16}$ presenting that the null hypothesis should be rejected. Therefore, the alternative hypothesis is accepted. It means that there is a slope of the line which was initially supposed to be zero. Based on this equation, the compressive strength of concrete can be computed among this frequency range.

$$Y = -9804.639 + 3.474\,(X) + 399.7 \qquad (7)$$

Additionally, a Quantile-Quantile plot (Q-Q plot) is used to assess whether a dataset follows a particular probability distribution, such as the normal distribution. It compares the quantiles of the dataset with the quantiles of a theoretical distribution, typically plotted along the x-axis and y-axis, respectively. In a Q-Q plot, if the points approximately follow a straight line, it suggests that the dataset is consistent with the theoretical distribution. Deviations from the straight line indicate departures from the assumed distribution. Q-Q plots are particularly useful for identifying deviations from normality in a dataset, which is important for making valid statistical inferences when using parametric methods like linear regression or Analysis of Variance (ANOVA).

DOI: 10.3844/ajeassp.2024.102.115

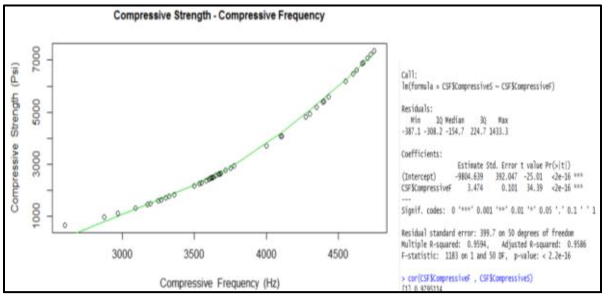

Fig. 4: Linear regression for compressive strength-compressive frequency

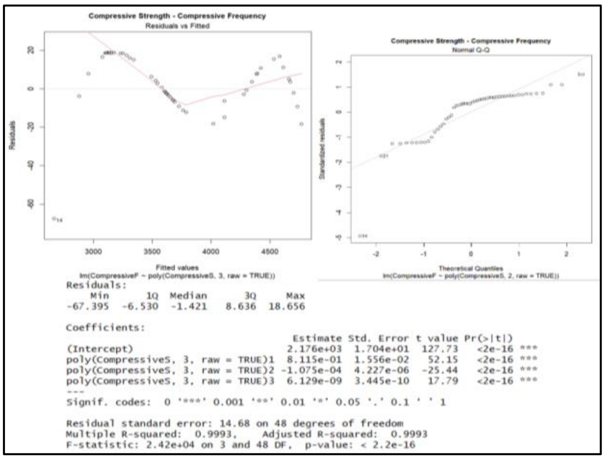

Fig. 5: Compressive strength-frequency: Residual and normal Q-Q plot

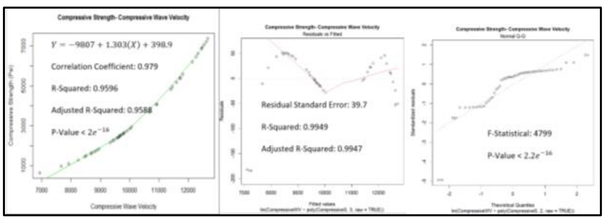

Fig 6: Compressive strength-compressive wave velocity: Regression, residual and normal Q-Q plot

Figure 5, the residual, Q-Q plots and the results for the compressive strength-frequency model are shown. The residual plot presents that there is no randomly distributed data. In other words, this model has a nonlinear relationship. The Q-Q plot approves nonlinearity since it does not have a completely uniform distribution. This model can be declared to have a heavy-tailed distribution pattern. Both the R-squared and adjusted R-squared exhibit exceptional accuracy, surpassing 99%. Figure 6 shows the regression criteria of compressive strength-compressive wave velocity for which the correlation coefficient is 0.979. The rejection of the null hypothesis is warranted by the low p-value (below 0.05), indicating the acceptance of the model equation (Fig. 6). Figure 7, the compressive velocity and frequency have very good regression. In other words, the correlation coefficient tends to be 1.00 and the R-squared error is 1.00 as well. The Q-Q plot has a lighted tail trend meaning that the values are smaller than the expected predicted values.

In the ICA method, the training data set constitutes 80%, with the remaining 20% allocated for testing. Random samples are generated using the rand perm command, producing row vectors of data sets. Subsequently, the network data set, training and cost function are defined. In the context of defining a regression model, a comparison is made between the real output and the network output. The Mean Squared error parameters have been defined to find out this error percentage and the correlation coefficient of the data set is calculated based on the linear regression.

The trained neural network demonstrates promising performance on both the training and testing datasets. Specifically, the Mean Squared Error (MSE) values for the compressive frequency-strength and compressive wave velocity datasets are 0.0039 for both the training and testing datasets (as illustrated in Figs. 8 and 10). These low MSE values indicate that the model accurately captures the relationships between the input features and the corresponding output variables. Additionally, the correlation coefficients for the training and testing datasets are 0.9942, as depicted in Figs. 9 and 11, respectively. These high correlation coefficients signify strong correlations between the actual output values and the predictions made by the neural network model.

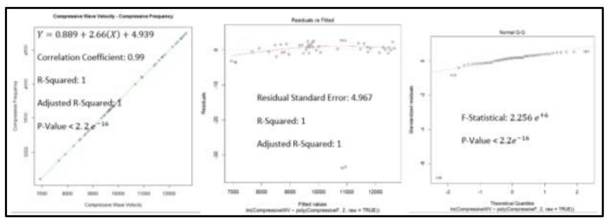

Fig. 7: Compressive frequency-compressive wave velocity: Regression, residual and normal Q-Q plot

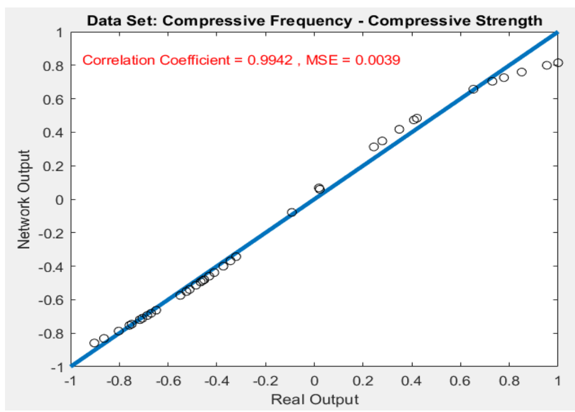

Fig. 8: Imperial competitive algorithm method for linear regression, compressive frequency-strength

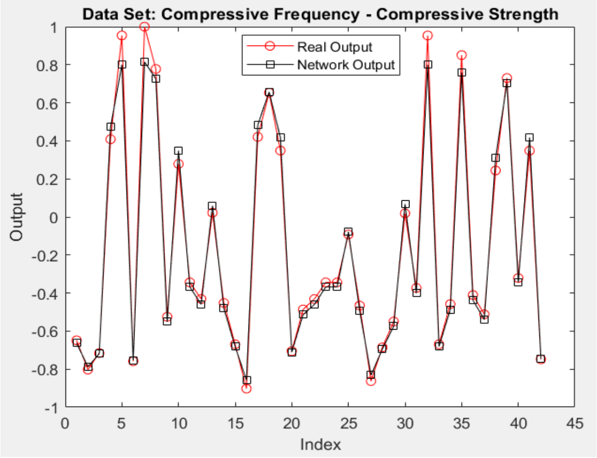

Fig. 9: Imperial competitive algorithm method-prediction of real-network, compressive frequency-strength

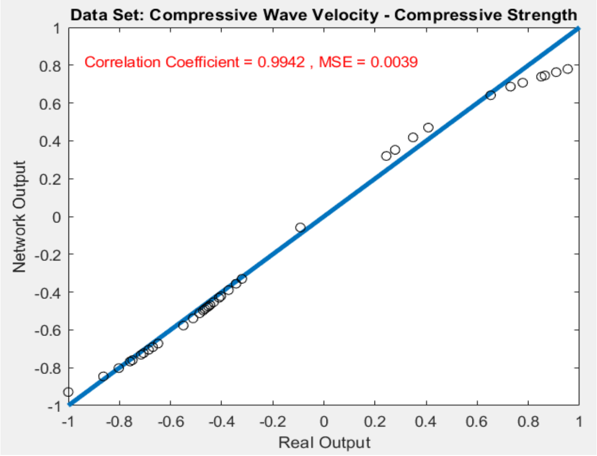

Fig. 10: Imperial competitive algorithm method for linear regression, compressive wave velocity-strength

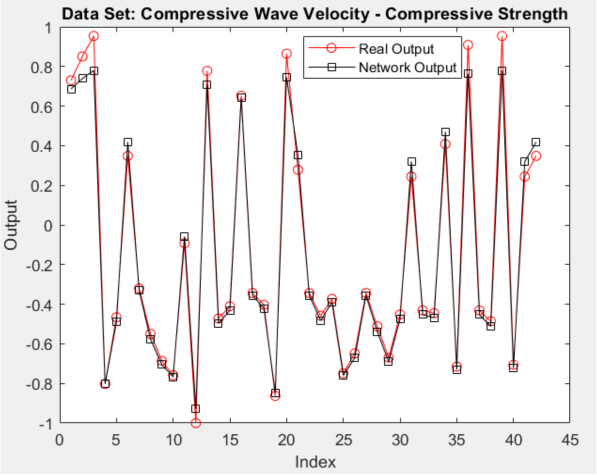

Fig. 11: Imperial competitive algorithm method-prediction of real-network, compressive wave velocity-strength

The effectiveness of the trained neural network model is further underscored by visualizations. A plot comparing the real output values with the network's predicted output values for the training dataset vividly demonstrates the model's capability to approximate the target function. This plot serves as tangible evidence of the model's accuracy and proficiency in capturing the underlying patterns within the data. Furthermore, a Quantile-Quantile (Q-Q) plot provides a comprehensive view of the correlation between the real output and the network output across different quantiles of the dataset. This visualization confirms the model's consistency and accuracy across various segments of the dataset, reinforcing its reliability and effectiveness.

In conclusion, the results affirm the successful application of the Imperialist Competitive Algorithm (ICA) in training a neural network model for the provided dataset. Through its robust optimization capabilities, the ICA algorithm facilitated the creation of a neural network model that not only achieved accurate predictions but also established strong correlations between the input features and the output variables. These findings underscore the potential of the trained model for effective decision-making and predictive analysis in the domain.

Support Vector Machines (SVM)

SVM represents a potent and adaptable family of machine learning algorithms extensively employed in both classification and regression endeavors. Smola and Schölkopf (2004) developed the SVM. SVM is fundamentally a supervised learning algorithm adept at categorizing data points into distinct classes by identifying the optimal hyperplane that maximizes the separation between these classes. Essential to SVM are the "support vectors," which denote the data points positioned near the decision boundary and the algorithm strives to maximize the distance between these support vectors and the hyperplane.

Support Vector Machines (SVMs) present a robust and versatile approach to defect detection in concrete structures. These algorithms are well-suited for this task due to several key factors. Firstly, SVMs excel in binary classification tasks, making them adept at distinguishing between defective and non-defective concrete samples based on various features like texture, color, composition, or structural properties. Through the process of margin maximization, SVMs find the optimal hyperplane that best separates the data points of different classes while maximizing the margin, thus enhancing their discriminative power. Moreover, SVMs can handle non-linear relationships in the data using the kernel trick, which maps the data into a higher-dimensional feature space where it becomes linearly separable. This capability is crucial for capturing complex patterns and non-linear decision boundaries inherent in concrete defect detection tasks. Additionally, SVMs offer robustness to overfitting through regularization parameters, striking a balance between bias and variance to ensure generalization to unseen data. In concrete defect detection, where accurate classification of unseen samples is paramount, this robustness is invaluable. Furthermore, SVMs perform effectively in high-dimensional spaces, making them suitable for datasets with numerous features such as those encountered in concrete defect detection. Finally, SVMs provide interpretable decision boundaries, allowing domain experts to understand and interpret the model's decisions, which is essential for gaining insights into the factors contributing to concrete defects. In fact, SVMs offer a powerful and interpretable approach for defect detection in concrete structures, leveraging their ability to handle non-linear relationships, robustness to overfitting, effectiveness in high-dimensional spaces and interpretability to enhance the maintenance and safety assessment of infrastructure.

In the realm of classification, the SVM objective is to discern a hyperplane within an n-dimensional space that effectively segregates data points into their respective classes, ensuring maximal distance from the hyperplane. Termed "support vectors," these data points exert significant influence on the hyperplane's positioning due to their proximity, ultimately defining the classifier's margin. The pursuit of an optimal hyperplane involves selecting one with the maximum margin, representing the utmost separation between data points from both classes.

Hyperplanes serve as decisive boundaries for classifying data points, where those falling on either side are assigned to different classes, with the hyperplane's dimension contingent upon the number of features. Support vectors, being those in closest proximity to the hyperplane, play a pivotal role in determining its position and orientation. The removal of support vectors alters the hyperplane's location, underscoring their crucial role in SVM construction.

The SVM algorithm aims to maximize the margin between data points and the hyperplane, with hinge loss serving as the pivotal loss function. In scenarios where there is no misclassification, the model updates the gradient solely from the regularization parameter. However, in the event of misclassification, where the model erroneously predicts the class of a data point, the loss, in conjunction with the regularization parameter, is incorporated for gradient update. This comprehensive overview illuminates the key facets of SVM, providing insights into its classification mechanism and the pivotal role played by support vectors in optimizing model performance. For more details about using SVM in construction and civil engineering refer to (Damirchilo *et al*., 2021; Damirchilo, 2021; Smola and Schölkopf, 2024).

The provided Python script facilitates defect detection in concrete utilizing a statistical approach, particularly leveraging Support Vector Machines (SVMs) for pattern recognition. The script begins by importing essential libraries such as os, pandas, numpy and modules from scikit-learn. It then sets the working directory to the location where the data files are stored. Ranges for each defect category (control, void, corrosion) are defined based on various concrete properties like shear velocity, compressive velocity, frequency, modulus of elasticity, shear modulus and compressive strength. The load_dataset () function reads CSV files containing data for each defect category and combines them into a single dataset. The dataset is then split into training and testing sets using the train_test_split () function from scikit-learn. The train_model () function trains an SVM classifier using the training data. Evaluating the Model: The evaluate_model () function assesses the trained model's performance on the testing data and prints a classification report. The predict_defect_category () function takes input parameters for concrete properties and predicts the defect category (control, void, corrosion) based on the predefined ranges. The main function prompts the user to enter concrete property values, creates an input parameters list and predicts the defect category using the trained SVM model. The main () function orchestrates the entire process by calling the aforementioned functions in sequence. It loads the dataset, trains the SVM model, evaluates its performance and finally predicts the defect category based on user input. The main function is invoked to execute the defect detection process when the script is run as the main program. Overall, this script offers an automated approach to detect defects in concrete by employing SVM-based pattern recognition, providing a systematic method to classify concrete samples into different defect categories based on their properties.

Reinforced Concrete Defects Classification with Support Vector Machine

This research explores the application of SVM in the classification of defects in reinforced concrete structures. The defects under consideration include void, corrosion and debonding, with a specific range defined for each type. Notably, due to the close proximity of corrosion and debonding ranges, they are treated as a single corrosion group in our analysis. Support Vector Machine (SVM) was originally designed for binary classification tasks, where it separates data into two classes using a hyperplane in a high-dimensional space. However, there are strategies to extend SVMs for multi-class classification, such as the One-vs-All (OvA) and One-vs-One (OvO) approaches. Figure 12 represents the hyperplane and support vectors for three classes (corrosion, void and control) while considering two features (shear velocity and compressive strength).

In this research, we used the OvO method which compares each pair of classes. Each classifier is trained to distinguish between two classes. In the OVO method, the resulting class is obtained by majority votes of all classifiers. Table 3 represents an example of how SVM compares 3 classes and selects corrosion with a majority vote of 2.

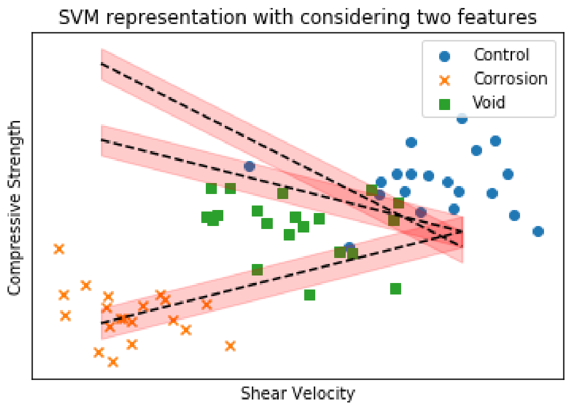

Fig. 12: Representation of classification of corrosion, void and control based on two features

Table 3: Multi-class classification based on OVO method representation

Class	Corrosion vs void	Corrosion vs control	Void vs control	Total
Corrosion	1	1	0	2
Void	1	0	0	1
Control	0	1	0	1

Table 4: Classification metrics for defects classes in reinforced concrete

	Metrics		
Defect category	Precision	Recall	F1-score
Control	0.50	0.50	0.50
Corrosion	0.50	1.00	0.67
Void	0.00	0.00	0.00

Table 5: Representing the SVM classification of defects in reinforced concrete structures

Features	Scenario 1	Scenario 2	Scenario 3
Shear velocity	4000	6500	9000
Compressive velocity	5000	9000	130000
Shear frequency	750	2000	3000
Compressive frequency	2100	3000	5000
Young's modulus	1580	4000	6000
Shear modulus	300	1000	2000
Compressive strength	2895	5000	7000
Defect category	Corrosion	Void	Control

The primary objective of this study is to leverage SVM to classify defects based on seven key features of reinforced concrete. These features encompass shear velocity, compressive velocity, shear frequency, compressive frequency, young modulus, shear modulus and compressive strength. The SVM model categorizes each defect into one of three groups: Void, corrosion, or a control group representing the absence of defects.

The data analysis is performed using the Python programming language, with the SVM modeling facilitated by the scikit-learn library. The dataset utilized for this study is presented in Table 2 and the data is split into training and test sets using the train_test_split function from scikit-learn. Specifically, 80% of the data is allocated for training, while the remaining 20% is reserved for testing.

The results of the SVM classification are evaluated using precision, recall and F1-score, as outlined in Table 4.

Precision serves as a metric for assessing the accuracy of positive predictions, while recall measures the classifier's ability to correctly identify positive cases in the dataset. The F1-score, regarded as the harmonic mean of precision and recall, provides a comprehensive evaluation of the model's performance.

Table 5 depicts three scenarios for presenting values of seven features and SVM detects defects in each scenario based on these feature values. The defect categories in scenarios 1, 2 and 3 are corrosion, void and control, respectively.

The absence of a comprehensive and complete comparison of results from different algorithms and the lack of comparison with other algorithms in this study could be attributed to various factors. Firstly, the research appears to have primarily focused on specific Artificial Intelligence (AI) and Machine Learning (ML) methods, such as linear regression, Imperial Competitive Algorithm (ICA) and Support Vector Machines (SVM), for analyzing Impact Echo test data to classify defects in reinforced concrete structures. The primary aim was to assess the effectiveness of these selected methods rather than conducting a broad comparison with alternative algorithms. Secondly, conducting a thorough comparison of multiple algorithms requires significant resources, including time, computational power and expertise. Given the complexity of the study's methodology and the need for detailed analysis and validation, a prioritization of in-depth examination of a few selected algorithms over a broader comparison is made by the researchers. Thirdly, the study is designed with specific research objectives and a defined scope, focusing on the development and evaluation of AI and ML techniques for defect classification using nondestructive testing methods. Extending the comparison to a wide range of algorithms could have exceeded the intended scope. Finally, the researchers relied on existing literature and established methods in the field of nondestructive testing and defect classification in reinforced concrete structures. Consequently, the proposed algorithms have been evaluated against these established methods rather than conducting a comprehensive comparison with alternative algorithms.

Conclusion

This research studies different statistical methods, machine learning and neural network methods to determine the type of defects inside reinforced concrete structures. By using the methodologies described in this study, researchers can predict the type of defects using nondestructive test methods. On the top of the explanations, the results can be ordered as follows.

The impact Echo test can be employed to accurately obtain the required data for defect detection of existing concrete structures.

The paper employed linear regression analysis to investigate the relationship between compressive strength and frequency in concrete, revealing high correlation coefficients exceeding 98% and providing a mathematical equation (Eq. 7) to represent the relationship.

Q-Q plots were utilized to assess the normality of the dataset and identify deviations from expected distributions, enhancing understanding of the data's characteristics, including nonlinearity and distribution patterns and validating statistical inferences drawn from the linear regression models. These insights contributed to the study's findings and provided practical implications for predicting concrete properties based on frequency and velocity parameters.

The ICA method with the trained neural network exhibits promising performance on both training and testing datasets, with low MSE values of 0.0039 for compressive frequency-strength and compressive wave velocity datasets. High correlation coefficients of 0.9942 for both training and testing datasets indicate strong correlations between actual output values and predictions made by the neural network model.

Visualizations further underscore the effectiveness of the trained neural network model, with a plot comparing real and predicted output values for the training dataset demonstrating the model's capability to approximate the target function. Additionally, a Quantile-Quantile (Q-Q) plot provides a comprehensive view of the correlation between real output and network output across different quantiles of the dataset, confirming the model's consistency and accuracy. These results affirm the successful application of the Imperialist Competitive Algorithm (ICA) in training a neural network model, indicating its potential for effective decision-making and predictive analysis in the domain.

The support vector machine method classifies the category of defects based on impact echo results and displays the defect’s type per user-input data.

Acknowledgment

The authors would like to thank their colleagues for their support and contributions.

Funding Information

The authors have not received any financial support or funding to report.

Author’s Contributions

Sajjad Sayyar Roudsari, Armaghan Shalbaftabar, Farshid Damirchilo, Rohollah Taslimian, Taher Abu-Lebdeh, Sameer Hamoush and Sun Yi: I agree to the proposed new authorship shown in section 4/and the addition/removal* of my name to the authorship list/and the proposed change in corresponding author.

Ethics

This article is an original research paper. There are no ethical issues that may arise after the publication of this manuscript.

Future Work

This research can be extended to detect internal cracks and crack propagation of existing reinforced concrete structures.

References

Akossou, A. Y. J., & Palm, R. (2013). Impact of data structure on the estimators R-square and adjusted R-square in linear regression. *Int. J. Math. Comput*, *20*(3), 84-93. https://www.researchgate.net/publication/289526309

Atamturktur, S. (2011, April). Defect detection in concrete members. In *Dynamics of Civil Structures, Volume 4: Proceedings of the 28th IMAC, A Conference on Structural Dynamics, 2010* (155-175). New York, NY: Springer New York. https://doi.org/10.1007/978-1-4419-9831-6_18

Beben, D., Mordak, A., & Anigacz, W. (2013). Ground penetrating radar application to testing of reinforced concrete beams. *Procedia Engineering*, *65*, 242-247. https://doi.org/10.1016/j.proeng.2013.09.037

Brilakis, I., German, S., & Zhu, Z. (2011). Visual pattern recognition models for remote sensing of civil infrastructure. *Journal of Computing in Civil Engineering*, *25*(5), 388-393. https://doi.org/10.1061/(ASCE)CP.1943-5487.0000104

Carino, N. J. (2001). The Impact-Echo Method: An Overview. In ASCE Library. https://doi.org/10.1061/40558(2001)15

Collins, R. (1995). Nondestructive Testing of Materials (R. Collins, Ed.; 1st Ed., Vol. *8*). IOS Press. ISBN-10: 9789051992397.

Damirchilo, F., Hosseini, A., Mellat Parast, M., & Fini, E. H. (2021). Machine learning approach to predict international roughness index using long-term pavement performance data. *Journal of Transportation Engineering, Part B: Pavements*, *147*(4), 04021058. https://doi.org/10.1061/JPEODX.0000312

Damirchilo, F. (2021) Use of Machine Learning and Data Science on Infrastructure Transportation and Construction Projects. *Arizona State University*. https://keep.lib.asu.edu/items/168518

Dawood, T., Zhu, Z., & Zayed, T. (2018). Computer vision–based model for moisture marks detection and recognition in subway networks. *Journal of Computing in Civil Engineering*, *32*(2), 04017079. https://doi.org/10.1061/(ASCE)CP.1943-5487.0000728

Deschepper, E., Thas, O., & Ottoy, J. P. (2006). Regional residual plots for assessing the fit of linear regression models. *Computational Statistics and Data Analysis*, *50*(8), 1995-2013. https://doi.org/10.1016/j.csda.2005.03.008

Hoła, J., & Runkiewicz, L. (2018). Methods and diagnostic techniques used to analyse the technical state of reinforced concrete structures. *Structure and Environment*, *10*(4), 309-337. https://doi.org/10.30540/sae-2018-030

Hong, S., Yoon, S., Kim, J., Lee, C., Kim, S., & Lee, Y. (2020). Evaluation of condition of concrete structures using ultrasonic pulse velocity method. *Applied Sciences*, *10*(2), 706. https://doi.org/10.3390/app10020706

Hugenschmidt, J. (2002). Concrete bridge inspection with a mobile GPR system. *Construction and Building Materials*, *16*(3), 147-154. https://doi.org/10.1016/S0950-0618(02)00015-6

Iván, J., & Carlos, J. (2015). Gráfico Q-Q Modificado Para Grandes Tamaños de Muestra. *Comunicaciones En Estadística*, *8*(2), 163-172. https://doi.org/10.15332/s2027-3355.2015.0002.02

Jäntschi, L., Pruteanu, L. L., Cozma, A. C., & Bolboacă, S. D. (2015). Inside of the Linear Relation between Dependent and Independent Variables. *Computational and Mathematical Methods in Medicine*, *2015*(1), 360752. https://doi.org/10.1155/2015/360752

Jiang, S., Deng, W., Ooi, E. T., Sun, L., & Du, C. (2024). Data-driven algorithm based on the scaled boundary finite element method and deep learning for the identification of multiple cracks in massive structures. *Computers and Structures*, *291*, 107211. https://doi.org/10.1016/j.compstruc.2023.107211

Johnson, M. R., & Pessiki, S. P. (1993). *Nondestructive evaluation of in-place concrete strength in plate structures by the impact-echo method* (Master's thesis, Lehigh University). https://core.ac.uk/download/pdf/228657023.pdf

Kaveh, A., & Talatahari, S. (2010). Optimum design of skeletal structures using imperialist competitive algorithm. *Computers and Structures*, *88*(21-22), 1220-1229. https://doi.org/10.1016/j.compstruc.2010.06.011

Kuchipudi, S. T., & Ghosh, D. (2024). Automated detection and segmentation of internal defects in reinforced concrete using deep learning on ultrasonic images. *Construction and Building Materials*, *411*, 134491. https://doi.org/10.1016/j.conbuildmat.2023.134491

Lopes, S. M. R., & Nepomuceno, M. (1997, July). Penetration Resistance Tests on High Strength Concrete. In 1st International Conference on High Strength Concrete. *American Society of Civil Engineers*, (425-433). https://ubibliorum.ubi.pt/handle/10400.6/4548

Mohammadi-Ivatloo, B., Rabiee, A., Soroudi, A., & Ehsan, M. (2012). Imperialist competitive algorithm for solving non-convex dynamic economic power dispatch. *Energy*, *44*(1), 228-240. https://doi.org/10.1016/j.energy.2012.06.034

Nanekar, P., Jothilakshmi, N., & Raj, B. (2019). Nondestructive Evaluation of Corrosion: Case Studies I. *Non-Destructive Evaluation of Corrosion and Corrosion-Assisted Cracking*, 1st Ed., 75-100. https://doi.org/10.1002/9781118987735.ch3

Nepomuceno, M. C., & Lopes, S. M. (2017, October). Analysis of within-test variability of non-destructive test methods to evaluate compressive strength of normal vibrated and self-compacting concretes. *In IOP Conference Series: Materials Science and Engineering*, 245(*3*), 032025. IOP Publishing. https://doi.org/10.1088/1757-899X/245/3/032025

Oh, B. D., Choi, H., Chin, W. J., Park, C. Y., & Kim, Y. S. (2023). Void Detection inside Duct of Prestressed Concrete Bridges Based on Deep Support Vector Data Description. *Applied Sciences*, *13*(10), 5981. https://doi.org/10.3390/app13105981

Pogliani, L., & De Julián-Ortiz, J. V. (2005). Residual plots and the quality of a model. *Match-Communications in Mathematical and in Computer Chemistry*, *53*(1), 175-180. ISSN 0340-6253.

Rehman, S. K. U., Ibrahim, Z., Memon, S. A., & Jameel, M. (2016). Nondestructive test methods for concrete bridges: A review. *Construction and Building Materials*, *107*, 58-86. https://doi.org/10.1016/j.conbuildmat.2015.12.011

Ross, A., & Willson, V. L. (2018). Basic and advanced statistical tests: Writing results sections and creating tables and figures. *Springer*. ISBN-10: 9789463510868.

Roudari, S. S., Okore-Hanson, T., Hamoush, S. A., & Yi, S. (2020, March). GPR robotic assisted non-destructive evaluation of concrete structures-20196. *In Waste Management*. https://hal.science/hal-02559868/

Roudsari, S. S. (2020). *Destructive and Robotic Assisted Non-Destructive Evaluation of Concrete Structures* (Doctoral dissertation, North Carolina Agricultural and Technical State University).

Sadowski, Ł., & Hoła, J. (2022). *Non-destructive Diagnostics of Concrete Floors: Methods and Case Studies*. CRC Press. https://doi.org/10.1201/9781003288374

Sayyar-Roudsari, S., Hamoush, S. A., Szeto, T. M., & Yi, S. (2020). Using a 3D computer vision system for inspection of reinforced concrete structures. *In Advances in Computer Vision: Proceedings of the 2019 Computer Vision Conference (CVC)*, 2(*1*) 608-618. Springer International Publishing. https://doi.org/10.1007/978-3-030-17798-0_49

Shah, A. A., Alsayed, S. H., Abbas, H., & Al-Salloum, Y. A. (2012). Predicting residual strength of non-linear ultrasonically evaluated damaged concrete using artificial neural network. *Construction and Building Materials*, *29*, 42-50. https://doi.org/10.1016/j.conbuildmat.2011.10.038

Słoński, M., Schabowicz, K., & Krawczyk, E. (2020). Detection of flaws in concrete using ultrasonic tomography and convolutional neural networks. *Materials*, *13*(7), 1557. https://doi.org/10.3390/ma13071557

Sugimoto, K., Sugimoto, T., Utagawa, N., Kuroda, C., & Kawakami, A. (2018). Detection of internal defects of concrete structures based on statistical evaluation of healthy part of concrete by the noncontact acoustic inspection method. *Japanese Journal of Applied Physics*, *57*(7S1), 07LC13. https://doi.org/10.7567/JJAP.57.07LC13

Smola, A. J., & Schölkopf, B. (2004). A tutorial on support vector regression. *Statistics and Computing*, *14*, 199-222. https://doi.org/10.1023/B:STCO.0000035301.49549.88

Taslimian, R., Noorzad, A., & Maleki Javan, M. R. (2015). Numerical simulation of liquefaction in porous media using nonlinear fluid flow law. *International Journal for Numerical and Analytical Methods in Geomechanics*, *39*(3), 229-250. https://doi.org/10.1002/nag.2297

Taslimian, R., Noorzad, A., & Maleki Javan, M. R. (2023). Numerical analysis of liquefaction phenomenon considering irregular topographic interfaces between porous layers. *Journal of Earthquake Engineering*, *27*(5), 1095-1109. https://doi.org/10.1080/13632469.2022.2038727

Taslimian, R., Noorzad, A., & Noorzad, A. (2012). Modeling saturated porous media with elasto-plastic behavior and non-Darcy flow law considering different permeability coefficients. *In 15th World Conference on Earthquake Engineering*. https://hal.science/hal-04362537/

Van Trees, H. L., & Bell, K. L. (2007). Improved Bounds on the Local Mean Square Error and the Bias of Parameter Estimators. https://doi.org/10.1109/9780470544198.ch18

Vapnik, V. (1998). The support vector method of function estimation. *In Nonlinear Modeling: Advanced Black-Box Techniques*, (pp. 55-85). Boston, MA: Springer us. https://doi.org/10.1007/978-1-4615-5703-6_3

Zhao, G., Zhang, D., Zhang, L., & Wang, B. (2018). Detection of defects in reinforced concrete structures using ultrasonic nondestructive evaluation with piezoceramic transducers and the time reversal method. *Sensors*, *18*(12), 4176. https://doi.org/10.3390/s18124176